

**HYBRID NUMERICAL TREATMENT OF TWO-FLUID PROBLEMS  
WITH PASSIVE INTERFACES**

N. G. COGAN \*

---

\*DEPARTMENT MATHEMATICS, FLORIDA STATE UNIVERSITY, 208 LOVE BUILD-  
ING, TALLAHASS, FL 32306-4510, E-MAIL: COGAN@MATH.FSU.EDU, FAX: 850.644.7196

**Abstract.** We consider the coupled motion of a passive interface separating two immiscible fluids of different viscosities. There are several applications, such as biofilm disinfection, where the velocity of the two fluids as well as the interface is needed to determine the transport of diffusing substances. In this investigation, we use a hybrid approach which employs the Boundary Integral Method to determine the interface velocity and the method of Regularized Stokeslets to determine the velocity elsewhere in the domain.

Our approach capitalizes on the strengths of the two methods yielding an intuitive, efficient method for determining the velocity of a two fluid system throughout the domain. The main result of the presented method is the extension to two-fluid systems with varying viscosity. We describe the results of three numerical simulations designed to test the numerical method and motivate its use.

**Keywords:** Two-Fluid, Boundary Integral Method, Regularized Stokeslets, Biofilm

**1. Introduction.** We consider the dynamics of two immiscible fluids separated by a passive interface. The motion of both fluids is assumed to be dominated by viscosity and described mathematically by the incompressible Stokes equations. In the absence of a background flow, the fluids move because of stress differences at the interface. Due to the linearity of Stokes equations, the dynamics with a background flow is the superposition of the motion due to jump in the traction across the interface and the background motion of the fluids.

Even when the fluid equations are linear, the coupling between two fluids renders the full system nonlinear. Moreover, the interface between the two fluids is typically heterogeneous and not aligned with a regular grid complicating numerical approximations. Several methods have been introduced to deal with this problem including finite element methods and immersed interface methods. In the former, the main difficulty is that the domain is not stationary requiring substantial computation in order to triangulate the domain. In the latter, stencils points and weights are changed, typically using a priori jump conditions, to maintain second order accuracy in discretizations [11, 12, 14]. This can also be problematic for a dynamic interface even when the interface is passive rather than elastic.

The boundary integral method (BIM) exploits the linearity of the basic flows to translate the differential equations to integral equations. This method has several advantages including reduction in the dimensionality of the problem, ability to handle generic interfaces and incorporation of different material properties [17, 6]. The integral equation can be used to solve for the velocities at every point in the domain. In particular, the velocity of control points describing the interface can be determined as well as those at grid points on a superimposed regular grid.

Although using the BIM equations to determine the velocity away from the grid seems to be an attractive method to couple the fluid motion to the motion of diffusing substances, in practice the computational time slows down the implementation. To avoid this, we use the method of Regularized Stokeslets [4] to determine the velocities away from the interface once the interface velocity is obtained. This method is second-order accurate for points away from the interface. Near the interface the error is linear; however, the velocity found from BIM is second-order accurate at the interface. The method described here is a hybrid approach using BIM to determine the interface velocity and Regularized Stokeslets to determine the velocity elsewhere capitalizing on the effectiveness of each method. The focus of this report is on the development when the viscosity of each fluid may substantially different rather than the application of the developed algorithms which will be described elsewhere.

We organize the manuscript as follows: the first sections introduce the notation,

governing equations and briefly describes the development of the numerical methods; we then focus on several simulations aimed at validating the numerical methods and finally summarize the results.

**2. Numerical Methods.** The boundary integral method for treating fluid problems in various parameter regimes has been extensively studied in the past several decades [8, 15, 6]. The method relies on the existence of a Green's function for the PDE operators. The immediate practicality of this method is apparent for fluids that can be treated as inviscid or as Stokes fluids [16, 8, 11, 1]. In either of these cases Greens functions for various domains are readily obtained.

The main idea behind BIM is to use a version of the Lorenz reciprocal relation [13] to recast the governing PDE's as boundary integrals equations. In general the reciprocal identity allows one to obtain information about a given flow,  $\mathbf{U}$  using information about another known flow,  $\mathbf{U}'$ . Because the flow field for a viscous fluid with a singular force can be calculated directly the unknown flow can then be related to that of a known flow. Once the reciprocal relation is derived the governing equations can be recast as integral equations whose domain is the boundary between the fluids.

**2.1. Model Equations.** We consider the coupled motion of two fluids of different viscosities. We assume that viscosity dominates both fluids, so the inertial terms may be neglected. The fluids occupy a region  $\Omega$  and are separated by a surface,  $\Gamma$ . We denote the two sub-regions as  $\Omega^{(1)}$  and  $\Omega^{(2)}$  for the external and internal fluids, respectively.

The dynamics of both fluids are governed by the incompressible Stokes equations

$$(2.1) \quad \nabla \cdot \sigma^{(*)} = 0$$

$$(2.2) \quad \nabla \cdot \mathbf{U}^{(*)} = 0,$$

where  $* = 1, 2$  denotes variables in the external and internal regions, respectively. Stokes equations describe conservation of momentum and mass with stress tensors  $\sigma^* = P^* \mathbf{I} + \mu^* (\nabla \mathbf{U}^* + \nabla \mathbf{U}^{*\mathbf{T}})$  contain both the hydrostatic pressures,  $P^*$ , and the viscous stresses proportional to the deformation gradient tensor.

By relating the unknown velocity  $\mathbf{U}^*$  to the flow induced by a singular force with intensity  $\mathbf{f}$  at a point  $\mathbf{x}_0$ ,  $\mathbf{U}'$  we reduce the partial differential equations in both sub-regions to a single integral equation that relates the bulk fluid velocity to the traction jump across the interface, denoted  $\Delta\sigma = (\sigma^{(1)} - \sigma^{(2)})$ , and the velocity at the interface (see [15] for details):

$$(2.3) \quad \begin{aligned} \mathbf{U}_j^{(1)}(\mathbf{x}_0) = & -\frac{1}{4\pi\mu^{(1)}} \int_{\Gamma} \Delta\sigma_{ik}\eta_k(\mathbf{x}) \mathbf{G}_{ij}(\mathbf{x}, \mathbf{x}_0) dl(\mathbf{x}) \\ & + \frac{1-\lambda}{4\pi} \int_{\Gamma} \mathbf{U}_i(\mathbf{x}) \mathbf{T}_{ijk}(\mathbf{x}, \mathbf{x}_0) \eta_k(\mathbf{x}) dl(\mathbf{x}), \end{aligned}$$

where  $\lambda = \frac{\mu^{(2)}}{\mu^{(1)}}$ . Equation (2.3) governs the  $j$ -th component of the external fluid velocity.

In a similar manner, we obtain an integral equation for the motion in  $\Omega^{(2)}$ ,

$$(2.4) \quad \begin{aligned} \mathbf{U}_j^{(2)}(\mathbf{x}_0) = & -\frac{1}{4\pi\mu^{(1)\lambda}} \int_{\Gamma} \Delta\sigma_{ik}\eta_k(\mathbf{x}) \mathbf{G}_{ij}(\mathbf{x}, \mathbf{x}_0) dl(\mathbf{x}) \\ & + \frac{1-\lambda}{4\pi\lambda} \int_{\Gamma} \mathbf{U}_i(\mathbf{x}) \mathbf{T}_{ijk}(\mathbf{x}, \mathbf{x}_0) \eta_k(\mathbf{x}) dl(\mathbf{x}). \end{aligned}$$

**2.2. Numerical Methods.** The general method begins by initializing the interface between the two fluids,  $\Gamma$ . We parametrize the coordinates of the interface by  $s$ ,  $\Gamma(x, y, t) = (x(s, t), y(s, t))$ . The interface is discretized into control points and Equations (2.3) and (2.4) are solved at each of the discrete points. We then use the method of regularized Stokeslets to determine the velocity at regular grid points. The velocities can then be used to determine the transport of a chemical throughout the domain.

In Equations (2.3) and (2.4), the kernel of the first integral is given in terms of a jump in the material stresses at the interface. This jump is assumed to be proportional to the mean curvature as in [15]  $\Delta\sigma = \gamma\eta\nabla\cdot\eta$ . Substituting this into the first integral on the right-hand-side of Equation (2.3) and expanding the Einsteinian notation we find that

$$\begin{aligned} & -\frac{1}{4\pi\mu^{(1)}} \int_{\Gamma} \Delta\sigma_{ik}\eta_k(\mathbf{x})\mathbf{G}_{ij}(\mathbf{x}, \mathbf{x}_0) dl(\mathbf{x}) = \\ & -\frac{\gamma}{4\pi\mu^{(1)}} \int_{\Gamma} (\mathbf{G}_{1j}\eta_1 + \mathbf{G}_{2j}\eta_2)\left(\eta_1\frac{\partial\eta_1}{\partial x} + \eta_2\frac{\partial\eta_2}{\partial y}\right) dl(\mathbf{x}), \end{aligned}$$

where  $\eta = (\eta_1, \eta_2)$ , denotes the components of the outward normal vector. The outward normals can be calculated using the parametrization of the interface. The curvature of the boundary  $\Gamma(s) = (x(s), y(s))$  is given by

$$(2.5) \quad \gamma = \frac{x_s y_{ss} - y_s x_{ss}}{(x_s^2 + y_s^2)^{(3/2)}}$$

The Green's function in two dimensions is,

$$(2.6) \quad \mathbf{G}_{ij}(\hat{\mathbf{x}}) = -\delta_{ij} \ln r + \frac{\hat{\mathbf{x}}_i \hat{\mathbf{x}}_j}{r^2}.$$

The stress tensor is,

$$(2.7) \quad \mathbf{T}_{ijk} = -4\frac{\hat{\mathbf{x}}_i \hat{\mathbf{x}}_j \hat{\mathbf{x}}_k}{r^4}.$$

Instead of using the free-space Green's function we could use the Green's function that enforces the zero-flow boundary condition by subtracting of image singularities if the domain is bounded (e.g. channel flow) [15].

**2.3. Implementation.** The velocity equations are Fredholm integrals of the second kind. A standard approach is Nyström's method which begins with a discretization of the boundary into  $N$  points [18]. Then we discretize the integral equation using a quadrature rule, we use the trapezoidal method, at the  $N$  points and invert the resulting matrix equation. Defining  $\mathbf{W} = (\mathbf{U}_1^{(1)}, \mathbf{U}_2^{(1)})$ , the system of integral equations can be written as

$$(2.8) \quad \mathbf{W} = \mathbf{b} + \frac{1-\lambda}{4\pi} \int_{\Gamma} \mathbf{K}\mathbf{W} dl(\mathbf{x}),$$

Where

$$\mathbf{b} = -\frac{1}{4\pi\mu^{(1)}} \left( \begin{array}{c} \int_{\Gamma} \gamma(\mathbf{G}_{11}\eta_1 + \mathbf{G}_{21}\eta_2)\left(\frac{\partial\eta_1}{\partial x} + \frac{\partial\eta_2}{\partial y}\right) dl(\mathbf{x}) \\ \int_{\Gamma} \gamma(\mathbf{G}_{12}\eta_1 + \mathbf{G}_{22}\eta_2)\left(\frac{\partial\eta_1}{\partial x} + \frac{\partial\eta_2}{\partial y}\right) dl(\mathbf{x}) \end{array} \right)^T,$$

and

$$\mathbf{K} = \begin{bmatrix} \mathbf{T}_{111}\eta_1 + \mathbf{T}_{112}\eta_2 & \mathbf{T}_{211}\eta_1 + \mathbf{T}_{212}\eta_2 \\ \mathbf{T}_{121}\eta_1 + \mathbf{T}_{122}\eta_2 & \mathbf{T}_{221}\eta_1 + \mathbf{T}_{222}\eta_2 \end{bmatrix}.$$

Applying the quadrature to Equation (2.8) yields a discrete system of the form

$$(2.9) \quad \mathbf{W}(\mathbf{x}_0) = \mathbf{b}(\mathbf{x}_0) + \frac{1-\lambda}{4\pi} \sum_{j=1}^n \mathbf{K}(\mathbf{x} - \mathbf{x}_0) \mathbf{W}(\mathbf{x}) \omega_j.$$

Evaluating this at the  $N$  control points leads to

$$(2.10) \quad \mathbf{W}(\mathbf{x}_{0,i}) = \mathbf{b}\mathbf{x}_{0,i} + \frac{1-\lambda}{4\pi} \sum_{j=1}^n \mathbf{K}(\mathbf{x}_{0,i} - \mathbf{x}_j) \mathbf{W}(\mathbf{x}_{0,i}) \omega_j.$$

This system can be inverted using any convenient iterative solver (i.e. gmres or conjugate gradient).

It should be noted that the kernels of the integrals are singular at the interface. Naive implementation can yield unstable numerical methods. We choose to regularize the kernels in a manner that is similar to that used in the method of Regularized Stokeslets. For that, we return to Equation 2.1 and replace the right-hand-side with a regularize force  $\mathbf{f}\phi^\epsilon$ ,

$$(2.11) \quad \nabla \cdot \sigma = \mathbf{f}_0 \phi_\epsilon(\mathbf{x} - \mathbf{x}_0)$$

$$(2.12) \quad \nabla \cdot \mathbf{U} = 0,$$

where  $\phi_\epsilon(\mathbf{x} - \mathbf{x}_0)$  denotes a cutoff or *blob* function. For the particular choice of  $\phi_\epsilon = \frac{3\epsilon^3}{2\pi(|\mathbf{x}|^2 + \epsilon^2)^{5/2}}$ , we find that the regularized free-space Green's function is,

$$(2.13) \quad \mathbf{G}_{ij} = -\mathbf{f}_0 \delta_{ij} \ln(\sqrt{r^2 + \epsilon^2} + \epsilon) - \frac{\epsilon(\sqrt{r^2 + \epsilon^2} + 2\epsilon)}{(\sqrt{r^2 + \epsilon^2} + \epsilon)^2(\sqrt{r^2 + \epsilon^2})},$$

here  $r = |\mathbf{x}|$  and  $\mathbf{x} = \mathbf{x} - \mathbf{x}_0$ .

The reciprocal relation becomes

$$(2.14) \quad \int_{\Omega} \mathbf{U}_j^{(1)}(\mathbf{x}) \phi^\epsilon dV(\mathbf{x}) = -\frac{1}{4\pi\mu^{(1)}} \int_{\Gamma} \Delta\sigma_{ik} \eta_k(\mathbf{x}) \mathbf{G}_{ij}^\epsilon(\mathbf{x}, \mathbf{x}_0) dl(\mathbf{x}) \\ + \frac{1-\lambda}{4\pi} \int_{\Gamma} \mathbf{U}_i(\mathbf{x}) \mathbf{T}_{ijk}^\epsilon(\mathbf{x}, \mathbf{x}_0) \eta_k(\mathbf{x}) dl(\mathbf{x}),$$

where the regularized stresses are given by

$$\mathbf{T}_{ijk} = -\delta_{ik} P_j^\epsilon(\mathbf{x}, \mathbf{x}_0) + \frac{\partial \mathbf{G}_{ij}^\epsilon}{\partial x_k} + \frac{\partial \mathbf{G}_{kj}^\epsilon}{\partial x_i}.$$

Cortez et. al [5] argue that the left-hand-side can be approximated by  $\mathbf{U}_j^{(1)}(\mathbf{x}_0)$  to order  $\mathcal{O}(\epsilon^2)$  so we solve Equation (2.8), with the regularized kernel.

With this completed we have the velocity of the interface at the discrete control points. We could proceed in a similar manner and find the velocity at each point in a regular lattice. Instead we use the method described in [4]. We do this in several steps first concentrating on the bulk fluid velocities away from the interface. Viewing

the discrete interface points as the location of singular forces applied to the bulk fluid, we determine the force that must be applied to obtain the velocity obtained above. Because Stokes equations are linear, the velocity at the point is a linear combination of the forces applied at each of the discrete points, therefore given the velocities a single matrix inversion yields the force (see [4] for details) which are used to determine the velocities. In a similar manner the velocities in the interior region are obtained.

### 3. Simulations.

**3.1. Steady Flow.** We first describe the numerical results of applying the method for a single time step to validate the implementation of Nyströms method as well as demonstrate the behavior of the method for systems with differing viscosities. We begin with a square domain located at  $(-2, 2) \times (-2, 2)$ . A fluid of viscosity  $\mu_{int}$  located at the interior a circle of radius one. The fluid outside of the circle has viscosity  $\mu_{ext}$ . We use methods described in [11] to derive an analytic solution to the problem with given forces. We parametrize the circle by  $\mathbf{x} = (\cos(\theta), \sin(\theta))$  and take the analytic solutions given in [4] and scale the pressure with the internal and external viscosities.

The analytic representation of the pressure and velocities

$$p(r, \theta) = \begin{cases} \mu_{ext} r^{-3} \sin(3\theta), & \text{for } r > 1, \\ \mu_{int} r^3 \sin(3\theta), & \text{for } r < 1, \end{cases}$$

$$u_1(r, \theta) = \begin{cases} \frac{1}{8} r^{-2} \sin(2\theta) - \frac{3}{16} r^{-4} \sin(4\theta) + \frac{1}{4} r^{-2} \sin(4\theta), & \text{for } r \geq 1, \\ \frac{3}{8} r^2 \sin(2\theta) + \frac{1}{16} r^4 \sin(4\theta) - \frac{1}{4} r^2 \sin(2\theta), & \text{for } r \leq 1, \end{cases}$$

$$u_2(r, \theta) = \begin{cases} \frac{1}{8} r^{-2} \cos(2\theta) + \frac{3}{16} r^{-4} \cos(4\theta) - \frac{1}{4} r^{-2} \cos(4\theta), & \text{for } r \geq 1, \\ \frac{3}{8} r^2 \cos(2\theta) - \frac{1}{16} r^4 \cos(4\theta) - \frac{1}{4} r^2 \cos(2\theta), & \text{for } r \leq 1, \end{cases}$$

are used in

$$[\sigma_{ij}] \eta_j = -f_i, \text{ for } i = 1, 2$$

Where the stress tensor  $\sigma$  is

$$\sigma_{ij} = -p \delta_{ij} + \mu \left( \frac{\partial u_i}{\partial x_j} + \frac{\partial u_j}{\partial x_i} \right),$$

to calculate the boundary forces.

For our calculations we prescribe the boundary forces at discrete points representing the boundary and solve Equation (2.8) to determine the boundary velocities. The velocities at the control points are used to determine the forces to apply to the fluid regions to match the calculated velocities which in turn is used to determine the external and internal velocities via the method of regularized Stokeslets. Because we are only considering the steady problem for prescribed boundary forces we do not need to use the curvature constitutive assumption to specify the boundary traction. Instead,  $\nabla \sigma_{ij} \eta_j = f_i$

To consider the convergence of the numerical approximation to the exact solution, we allow the the number of points discretizing the interface,  $N$ , to increase while the background grid used to determine the velocity away from the interface is fixed. Following [4], we measure the error along the line  $(x, 3/10)$ . We first consider the case where the viscosities are equal as in [4] (see Table 3.1). The velocity field and  $x$  and

TABLE 3.1  
Velocity Errors:  $\mu_1 = \mu_2 = 1$

# Boundary Points	$L_2$ error in $u_1$	$L_2$ error in $u_2$
$N = 50$	$2.99 \times 10^{-2}$	$3.14 \times 10^{-2}$
$N = 100$	$7.89 \times 10^{-3}$	$6.46 \times 10^{-3}$
$N = 200$	$1.83 \times 10^{-3}$	$1.03 \times 10^{-3}$
$N = 400$	$4.47 \times 10^{-4}$	$3.53 \times 10^{-4}$

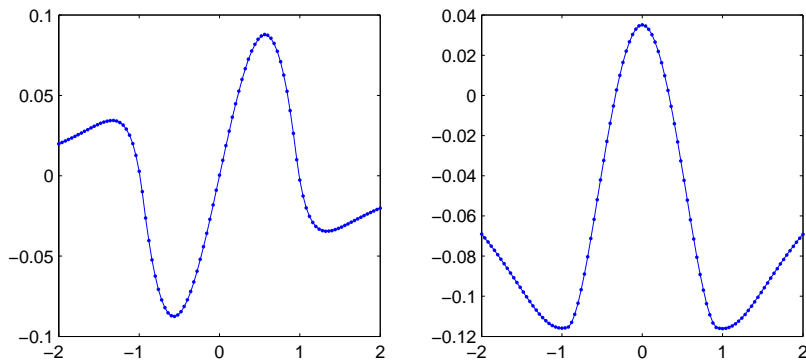


FIG. 3.1. Comparison of the analytic velocities (solid) and the numerical approximation (dotted) along the line  $(x, 3/10)$ . Left caption shows  $u_1$  while the right shows  $u_2$ . The background mesh has  $100 \times 100$  points and the boundary is discretized with 200 points. The solution is being approximated well except at the interface between the two fluids as in [4].

$y$ - components of the velocity along the line  $(x, 3/10)$  in Figure 3.1 indicate that the behavior is the similar as in [4].

Next, we consider the behavior when the viscosities of the two fluids are not equal. In general the convergence is similar to that obtained for equal velocities although as the ratio of the two viscosities becomes large, the convergence appears to become linear rather than quadratic. The results for different viscosities are summarized in Tables 3.2 and 3.3.

**3.2. Viscous Suctioning.** In the previous section we computed the approximate solution for a single time step. To determine the behavior of the numerical methods for a moving boundary, we choose to examine a problem that is similar to the well known Hele-Shaw problem with a singular sink term [2]. Here, we consider the flow of a two-fluid system where an initially circular blob of fluid with viscosity

TABLE 3.2  
Velocity Errors:  $\mu_1 = 1, \mu_2 = 2$

# Boundary Points	$L_2$ error in $u_1$	$L_2$ error in $u_2$
$N = 50$	$4.52 \times 10^{-2}$	$3.26 \times 10^{-2}$
$N = 100$	$1.19 \times 10^{-2}$	$1.39 \times 10^{-2}$
$N = 200$	$3.47 \times 10^{-3}$	$7.74 \times 10^{-3}$
$N = 400$	$1.36 \times 10^{-3}$	$4.17 \times 10^{-3}$

TABLE 3.3  
Velocity Errors:  $\mu_1 = 1, \mu_2 = 5$

# Boundary Points	$L_2$ error in $u_1$	$L_2$ error in $u_2$
$N = 50$	$2.68 \times 10^{-2}$	$5.06 \times 10^{-2}$
$N = 100$	$9.94 \times 10^{-2}$	$1.96 \times 10^{-2}$
$N = 200$	$4.78 \times 10^{-3}$	$8.90 \times 10^{-3}$
$N = 400$	$2.50 \times 10^{-3}$	$4.35 \times 10^{-4}$

$\mu_2$  is immersed in a viscous fluid of viscosity  $\mu_1$ . The circle is initially of radius one and centered at the origin. At time  $t = 0$ , we initiate a singular sink term at a point interior to the circle that draws the interior fluid out of the domain causing motion of the interface and the external fluid. This problem has been treated in many investigations (see [7] for analytic treatment and references). In general, in the absence of surface tension there is a singularity in finite time whenever  $\mu_2 > \mu_1$ . With small surface tension, the problem is regularized and various smooth solutions can be found depending on the location of the sink relative to the circle as well as the strength of the point-sink.

To include a singular sink term in our scheme, we consider the background flow that is the solution to:

$$\begin{aligned}\Delta \mathbf{U} &= \nabla p \\ \nabla \cdot \mathbf{U} &= q\delta(\mathbf{x} - \mathbf{x}_0),\end{aligned}$$

$\mathbf{U}_{suction} = \frac{\mathbf{x} - \mathbf{x}_0}{|\mathbf{x} - \mathbf{x}_0|}$ . This is added to the flow obtained due to the interface motion to give the motion of the interface.

The computational domain  $[-1.5, 1.5] \times [-1.5, 1.5]$  is discretized into a regular background grid with  $200 \times 200$  grid points. This initial interface is a circle of radius one centered at the origin. There are 150 regularly spaced control points. The surface tension,  $\gamma$ , is fixed at 0.001 for all simulations. In general, our method is able to capture the behaviors that are found analytically. The results for various simulations are shown in Figure 3.2.

**3.3. Advection.** One strength of the method described above, is efficient approximation of the velocity everywhere in the domain. This is important in transport problems, such as biofilm disinfection, where the main goal is to determine the concentration of biocide and nutrient as it moves in the bulk fluid and into the biofilm domain. Several models treat the biofilm as a viscous fluid with a viscosity that is substantially different than that of the external fluid [3, 10, 9].

The domain is a channel with a parabolic background flow. Within the channel a generic biofilm interface separates the biofilm fluid, with viscosity  $\mu_{biofilm}$  from the bulk fluid with viscosity  $\mu_{bulk}$ . Although biofilms display viscoelastic properties,

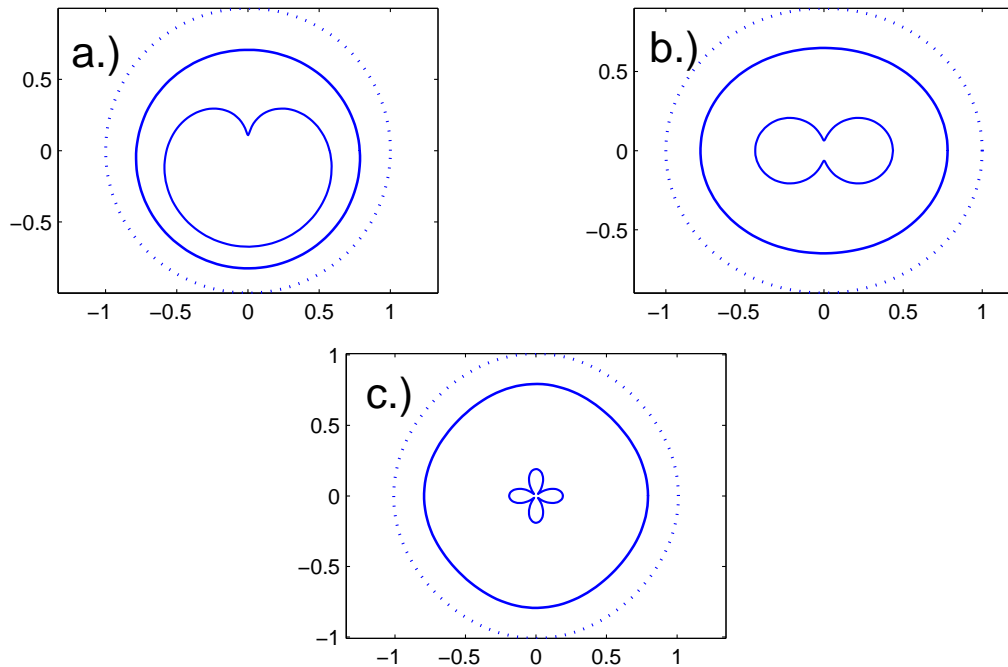


FIG. 3.2. Results for viscous suctioning. a.) Initially circular interface with singularity at  $(0, 0.1)$ . b.) To break the symmetry, we perturb the circle into an ellipse with major axis 1 and minor axis 0.9 in the  $y$ -direction. The singularity is placed at the origin. c.) To break the symmetry, we perturb the circle by adding a periodic fluctuation in the radius with amplitude .01. The singularity is placed at the origin. In all simulations the  $\mu_2 = 1$  and  $\mu_1 = 0.1$  and the initial interface is indicated with the dotted line while the other curves are shown after 100 and 250 time steps.

the relaxation time has been measured to be on the order of minutes [10]. Because transport of biocide within the biofilm typically takes place on a time scale of hours to days, we treat the biofilm as a viscous fluid immersed in a fluid of much less viscosity [9]. Measurements of biofilm viscosity indicate that the viscosities differ by several orders of magnitude [10]. We set  $\mu_{biofilm} = \mu_{bulk} \times 10^{-6}$  and impose a parabolic background flow which is altered by the presence of the biofilm. Following the methods described above, we determine the velocity of the interface and fluid in both the bulk and biofilm regions. This is used to track the advection and diffusion of a chemical whose concentration,  $C$ , is determined mathematically by a conservation law

$$\frac{\partial C}{\partial t} + (\mathbf{U} \cdot \nabla)C = D\Delta C,$$

where the concentration is fixed at  $C_0$  at the leading edge of the channel. No-flux and outflow conditions are applied at the channel walls and trailing edge of the channel.

Given the velocity at time  $t$  we determine the concentration at time  $t + \Delta t$  using upwinding and ADI to solve the discretized equation.

In Figure 3.3, we show the developing concentration contours as well as the biofilm/bulk fluid interface for various times. We plan to indicate the effects of including the motion of the biofilm in a future investigation.

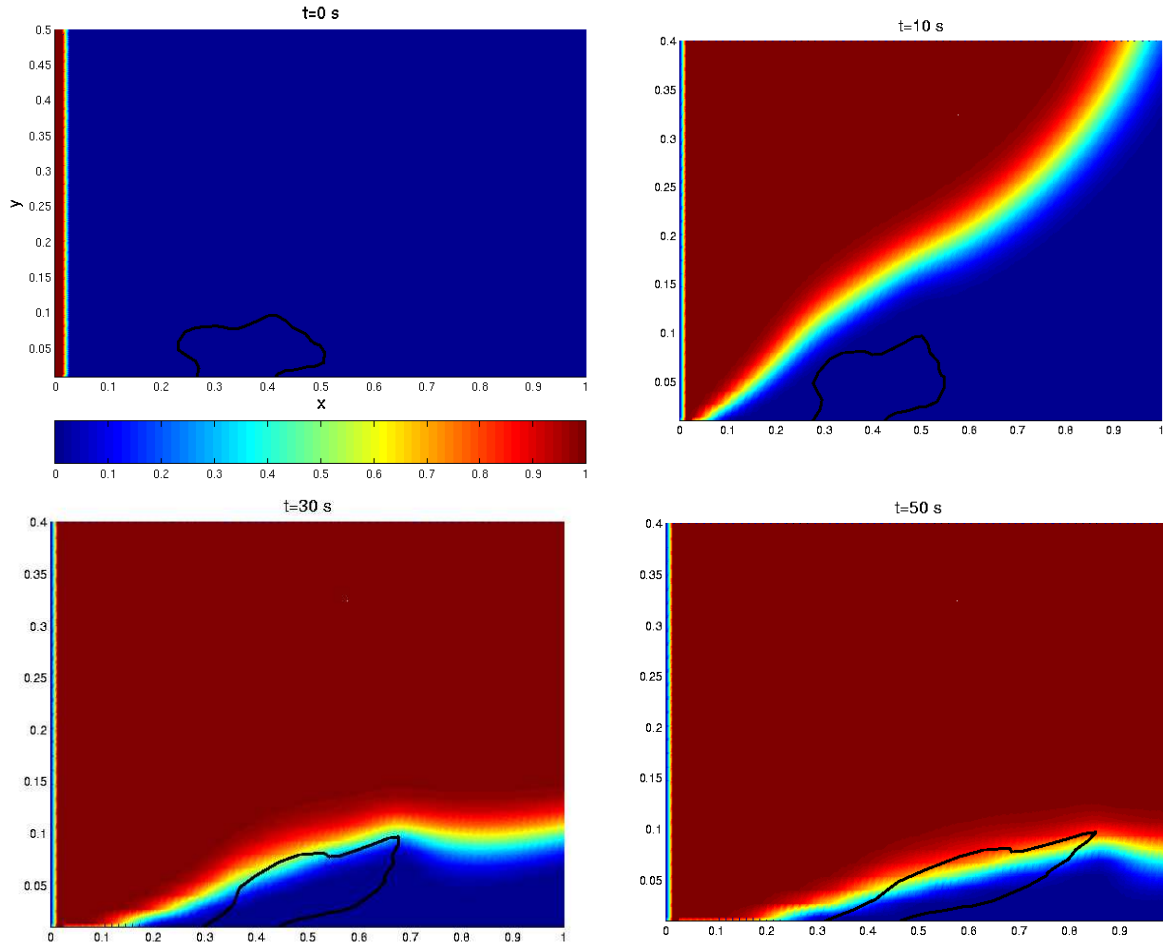


FIG. 3.3. Time dependent concentration profiles indicating the diffusion and advection of a chemical through the two-fluid domain. We show only part of the domain:  $[0, 1] \times [0, 0.4]$ . The dynamic fluid/biofilm interface is indicated in black and the concentration for all figures is indicated by the colorbar.

**4. Discussion.** This investigation describes the development of a hybrid method for numerically approximating the motion to two viscous fluids separated by an interface. The interface velocity at control points is determined by solving an integral equation. The velocity at the control points is then used as data to determine the flow outside and inside the interface using the method of Regularized Stokeslets. Our method capitalizes on the strengths of both of the methods, since Regularized

Stokeslets is an efficient method but leads to errors at the interface which is precisely where BIM is being applied.

To test the numerical method, we studied three different problems. The first was a static problem for which there is an analytic solution. We found that when the viscosities of the fluids are equal, the method behaves as in [4]. However, we have extended the treatment to case with differing viscosities. We then treated a viscous suctioning problem where we were able to capture the development of cusps as found analytically. Finally, we applied our method to determine the concentration of a chemical as it diffuses and advects throughout a channel filled with two immiscible fluids of extremely different viscosities.

This work is supported in part by DMS #0548511.

## REFERENCES

- [1] J. T. BEALE AND A. LAYTON, *On the accuracy of finite difference methods for elliptic problems with interfaces*. Submitted.
- [2] H. D. CENICEROS, T. Y. HOU, AND H. SI, *Numerical study of Hele-Shaw flow with suction*, *Physics of Fluids*, 11 (1999), pp. 2471–2486.
- [3] N. G. COGAN AND J. P. KEENER, *The role of the biofilm matrix in structural development*, *Mathematical Medicine and Biology*, 21 (2004), pp. 147–166.
- [4] R. CORTEZ, *The method of regularized stokeslets*, *SIAM J. Sci. Comput.*, 23 (2001), pp. 1204–1225.
- [5] R. CORTEZ, L. FAUCI, AND A. MEDOVIKOV, *The method of regularized stokeslets in three dimensions: Analysis, validation, and application to helical swimming.*, *Phys. Fluids.*, 17 (2005), pp. 1–14.
- [6] V. CRISTINI, J. BLAWZDZIEWICZ, AND M. LOEWENBERG, *Drop breakup in three-dimensional viscous flows*, *Phys. Fluids Letters*, 10 (1998), pp. 1781–1783.
- [7] L. J. CUMMINGS AND S. D. HOWISON, *Two-dimensional Stokes flow with suction and small surface tension*, *European Journal of Applied Mathematics*, 10 (1999), pp. 681–705.
- [8] T. Y. HOU, J. S. LOWENGRUB, AND M. J. SHELLEY, *Boundary integral methods for multi-component fluids and multiphase fluids*, *Journal of Computational Physics*, 169 (2001), pp. 302–362.
- [9] I. KLAPPER, *Effect of heterogeneous structure in mechanically unstressed biofilms on overall growth*, *Bulleting of Mathematical Biology*, 66 (2004), pp. 809–824.
- [10] I. KLAPPER, C. RUPP, R. CARGO, B. PURVEDORJ, AND P. STOODLEY, *Viscoelastic fluid description of bacterial biofilm material properties*, *Biotechnology and Bioengineering*, 80 (2002), pp. 289–296.
- [11] A. T. LAYTON, *An explicit jump method for the two-fluid stokes equations with an immersed elastic boundary*, Elsevier Science, (2006). Submitted.
- [12] R. J. LEVEQUE AND Z. LI, *Immersed interface methods for Stokes flow with elastic boundaries or surface tension*, *SIAM J. Sci. Comput.*, 18 (1997), pp. 709–735.
- [13] H. A. LORENZ, *Ein allgemeiner satz, die bewegung einer reibenden flussugkeit betreffend, nebst einigen anwendungen desselben*, *Abhand. Theor. Phys.*, 1 (1907), pp. 23–42.
- [14] A. MAYO, *Fast high order accurate solution of Laplace’s equation on irregular regions*, *SIAM J. Sci. Comput.*, 6 (1985), pp. 144–157.
- [15] C. POZRIKIDIS, *Boundary integral and singularity methods for linearized viscous flow*, Cambridge University Press, 1992.
- [16] ———, *Interfacial dynamics for stokes flow*, *Journal of Computational Physics*, 169 (2001), pp. 250–301.
- [17] ———, *Modeling and Simulation of Capsules and Biological Cells*, Chapman & Hall/CRC Press., 2003.
- [18] W. T. VETTERLING, S. A. TEUKOLSKY, W. H. PRESS, AND B. FLANNERLY, *Numerical Recipes in C: The Art of Scientific Computing*, Cambridge University Press, Cambridge, 2002.